Sustainable Food Technology

Accepted Manuscript

This article can be cited before page numbers have been issued, to do this please use: S. Khongtongsang, M. Fikry, S. Jafari, S. Chheng, I. Kijpatanasilp and K. Assatarakul, *Sustainable Food Technol.*, 2025, DOI: 10.1039/D5FB00648A.

ROYAL SOCIETY OF CHEMISTRY

View Article Online
DOI: 10.1039/D5FB00648A

Sustainability Spotlight Statement

This study highlights a sustainable microencapsulation approach using plant-based, biodegradable wall materials (gum arabic and resistant maltodextrin) to enhance the shelf life and stability of kratom leaf extract. By optimizing spray drying conditions, the process achieves efficient bioactive preservation through low-energy input and minimal resource use. The findings promote reduced food waste, extended product usability, and environmentally responsible formulation practices, supporting the advancement of green technologies in functional food and nutraceutical production.

View Article Online
DOI: 10.1039/D5FB00648A

Microencapsulation of Kratom Leaf Extract via Spray Drying: Impact of Inlet Temperature and Wall Materials on Stability and Shelf Life

Supanit Khongtongsang[a], Mohammad Fikry[a,b], Saeid Jafari[a], Sochannet Chheng[a,c],

Isaya Kijpatanasilp[a] and Kitipong Assatarakul[a]*

[a] Department of Food Technology, Faculty of Science, Chulalongkorn University, Bangkok, Thailand, 10330

[b] Department of Agricultural and Biosystems Engineering, Faculty of Agriculture, Benha University, Moshtohor,Toukh, Egypt, 13736

[d] Department of Food Chemical Engineering, Kampong Speu Institute of Technology, Kampong Speu 050601, Cambodia

*Corresponding author: Kitipong Assatarakul (Ph.D.);

Email: Kitipong.A@chula.ac.th; Tel. 0-2218-5328

View Article Online
DOI: 10.1039/D5FB00648A

Abstract

Microencapsulation offers a sustainable approach to improving the stability, functionality, and shelf life of bioactive compounds in food systems, reducing product waste and enhancing resource efficiency. The objectives of this study were to microencapsulate kratom leaf extract (KLE) using spray drying with gum arabic (GA) and resistant maltodextrin (RMD) at two inlet temperatures (150 and 160 °C), to evaluate the resulting microcapsules in terms of their physicochemical properties and assess bioactive retention, specifically total phenolic and flavonoid contents, as well as antioxidant activity, and to investigate stability and shelf-life prediction using kinetic modeling. The resulting microcapsules were evaluated for physicochemical properties, bioactive retention, antioxidant activity, and storage stability. Encapsulation yield ranged from 45.3–62.7%, while encapsulation efficiency was 70.8–83.5%, with GA at 160 °C showing the highest performance. Moisture content remained within 2.1–3.6%, and solubility ranged from 82.4–92.1%, with RMD providing greater solubility and lower residual moisture. Total phenolic content retention ranged from 65.2–79.6%, while total flavonoid retention was 61.4–76.8%. Antioxidant activity (DPPH inhibition) decreased by approximately 20% during processing, with GA at 160 °C preserving the highest activity. Storage studies showed that water activity remained below the stability threshold (a_w = 0.30), and first-order kinetic modeling predicted a shelf-life extension of up to 90 days under ambient conditions. Morphological analysis revealed spherical particles with smooth surfaces at 160 °C, whereas higher temperatures induced surface collapse and shrinkage. Overall, GA provided superior protection of phenolics and antioxidants, while RMD enhanced solubility and reduced residual moisture. The findings highlight the potential of using food-grade wall materials and

View Article Online
DOI: 10.1039/D5FB00648A

optimized spray drying conditions for scalable production of stable KLE microcapsules suitable for functional food and nutraceutical applications.

Keywords: Bioactive Compounds, Gum Arabic, Kratom Leaf, Microencapsulation, Spray-Drying

1. Introduction

Kratom (*Mitragyna Speciosa*) is a tropical plant belonging to the Rubiaceae family and is indigenous to Southeast Asia [1]. For hundreds of years, kratom has been utilized in various regions of Thailand and is known by several local names, including Thom, E-Thang, Ketum, Kratum-Koke, and Maeng Da Leaf [2]. Traditionally, fresh kratom leaves are commonly chewed or boiled to create a decoction. In contrast, dried leaves are typically smoked, brewed into tea, or consumed as an herbal drink, often with added honey and lemon [3]. Kratom has historically been used to relieve muscle fatigue and tiredness and as a herbal remedy for various common ailments, including diarrhea, diabetes, coughing, and hypertension. Additionally, it has been employed as an alternative to morphine or opium for treating drug addiction [4]. Some studies have shown that kratom exhibits a range of biological activities, such as anti-inflammatory, antinociceptive, antioxidant, and antimicrobial properties [5]. For these reasons, kratom leaves holds significant economic value, with fresh leaves selling for $8 to $10 per kilogram in Thai markets as of 2022 [6].

Extracting bioactive compounds from kratom leaves can enhance both the commercial value of the raw material and the profitability of its processing. Consequently, kratom leaves have garnered significant interest from researchers exploring both traditional and novel extraction techniques [7-10]. However, the stability of these extracted compounds can be compromised during processing and storage due to factors such as solvents, pH, temperature,

View Article Online
DOI: 10.1039/D5FB00648A

oxygen, light, and enzymes [11]. Hence, finding alternative methods to enhance the stability of these bioactive compounds during processing and storage is crucial.

The stabilization of bioactive compounds can be enhanced using microencapsulation technologies, such as spray drying [12], to improve their suitability for industrial applications and ensure their bioavailability. Spray drying is the preferred method for microencapsulation due to its cost-effectiveness, user-friendliness, and its ability to produce high-quality particles [13].

Spray drying microencapsulation is a technique used to protect essential substances from unwanted decomposition or reactions during storage [14]. This technology involves embedding active ingredients within microparticle matrices, creating a physical barrier between the active compound and the external environment while regulating its release. By encapsulating a bioactive compound in a biopolymer, the process shields it from oxygen, moisture, and other environmental factors, thus enhancing its stability. Additionally, it converts liquid solutions into powders, making them easier to handle [15].

Various encapsulating agents are employed in spray drying, including polysaccharides (such as starches, resistant maltodextrin **(**RMD**)**, corn syrups, and gum arabic (GA)), lipids (like stearic acid and mono- and diglycerides), and proteins (including gelatin, casein, milk serum, soy, and wheat). These substances are favored for their high-water solubility, low viscosity, neutral taste, and colorless solutions, making them widely utilized in the food industry (Jafari et al., 2023a).

On the other hand, using mathematical models is a highly effective approach to assess quality parameters at various stages of processing. Zero-order and first-order equations are frequently utilized to describe the changes in quality properties over time. Predictive models

View Article Online
DOI: 10.1039/D5FB00648A

have been previously developed to evaluate the shelf life of various products, by integrating the physical and phytochemical indicators [16].

Bioactive compounds from different plant leaves have been previously microencapsulated using spray drying technology [12, 14, 17-23].

Although kratom *(Mitragyna speciosa)* has been studied for its phytochemical composition and potential bioactivity [10, 24-26], no previous reports have investigated its microencapsulation using spray drying. Microencapsulation is crucial for protecting kratom extracts from degradation, improving stability, and facilitating reconstitution into functional products. However, knowledge remains limited regarding how different wall materials and processing conditions influence these outcomes. Therefore, the objectives of this study were to microencapsulate kratom leaf extract (KLE) using spray drying with gum arabic (GA) and resistant maltodextrin (RMD) at two inlet temperatures (150 and 160 °C), to characterize the resulting microcapsules in terms of their physicochemical properties, to evaluate bioactive retention including total phenolic and flavonoid contents as well as antioxidant activity, and to assess shelf-life using kinetic modeling.

2. Materials and Methods

2.1. Preparing kratom leaves extract (KLE)

Kratom leaves were sourced from a domestic market in Bangkok, Thailand. They were first rinsed with water to eliminate dirties, and then dried in a lab oven (Memmert, DO 6062, Germany) at a temperature of 60°C until their moisture content (MC) was reduced to less than 5%. The dried leaves were then ground and passed through a 50-mesh sieve.

For the preparing kratom leaf extract (KLE), three gram of the powdered leaves was immersed in 120 mL of solvent, following the modified procedures of [27]. The ultrasonic-assisted

View Article Online
DOI: 10.1039/D5FB00648A

extraction was performed using an ultrasonic homogenizer (UP400S Ultrasonic processor, Hielsher, Germany). The ultrasonic setting was: 400 W, 50**%** amplitude, 7 mm tip, pulse 30 s on/10 s off, 250 mL beaker, 50**%** immersion, ice bath **(**T<40°C**).** Vacuum evaporation was also conducted at 40°C under 100 mbar pressure until the extract reached a total solids content of approximately 15–20% (w/v), measured gravimetrically. Feasibility for encapsulation was confirmed by viscosity (<50 mPa·s at 25°C) and absence of precipitation, ensuring stable feed for spray drying. Based on preliminary experiments, the optimum extraction conditions included 90% (v/v) ethanol concentration, a 30-min extraction time, and an extraction ratio of 1:40 (w/v). According to the method described by [28], the extracts were centrifuged at 6000 × g **(**rotor radius 10 cm**)** for 15 min at 25 °C using a centrifuge (Centrifuge Kubota, series 6000, Japan). The supernatant was purified using Whatman No. 1 paper in order to eliminate coarse particles and then subjected to vacuum evaporation process utilizing a rotary evaporator (Oilbath B-485, BÜCHI, Switzerland) to ~20**%** solids **(**w/w**)**. The samples were stored in amber vials at 4°C for subsequent analysis.

2.2. Spray drying microencapsulation process

Microencapsulation was carried out using resistant maltodextrin (RMD; Fibersol-2, Matsutani, Japan), gum Arabic (GA; Agrigum, UK), and their combination as coating materials. Concentrations (w/w) were selected based on preliminary trials to achieve comparable feed viscosities (~20–40 mPa.s) while remaining within solubility limits: 20% for GA (to avoid excessive viscosity), 40% for RMD (optimal solubility), and a 1:1 blend (40% RMD with 20% GA) at equivalent total solids for comparison. All formulations were spray dried at inlet temperatures of 150 and 160 °C using a KLE-to-coating material ratio of 1:2 (w/w). The mixtures were prepared by combining KLE with the coating materials (Table 1) and stirring

View Article Online
DOI: 10.1039/D5FB00648A

continuously with a magnetic stirrer (SCILOGEX, SCI550-S, USA) for 10 min. The mixture was then homogenized with a high-speed blender (Ystral, model X10, Germany) at 11,000 rpm for 10 min. Feed solids were 20–40**%** w/w, viscosity 20–40 mPa·s, pump 10 mL/min, aspirator 90**%**, atomizing air 0**.**7 mm nozzle at 1 bar, feed at 25°C. The resulting solutions were processed through a spray dryer (BUCHI, B-290, Switzerland) set at inlet temperatures of 150 and 160 °C and an outlet temperature of 85-95 °C. The resulting powders were stored at -20°C for analysis of their properties (e.g., encapsulation yield, encapsulation efficiency, moisture content, water activity, water solubility, TPC, TFC, TTC, antioxidant activity via DPPH and FRAP) under different conditions. Figure (1) reveals the production flow chart of KLE microcapsules of bioactive compounds extracted from kratom leaves.

2.3. Calculation of the encapsulation yield and efficiency

Following the procedure of [29], the encapsulation yield (%) was determined and calculated using the following equation (Eq. 1):

$$Encapsulation\ Yield\ (\%) = \frac{m_{capsules,\ collected}}{m_{soilds,\ initial}} x100 \quad (1)$$

where $m_{capsules,\ collected}$ is the total mass of KLE microcapsules collected from the spray dryer, and $m_{solids,\ initial}$ is the mass of total solids in the feed before drying.

To calculate the percentage of encapsulation efficiency, the total bioactive compounds were measured first. A sample of 0.1 g of KLE encapsulated powder was dissolved in 1 mL of a mixed solution (ethanol: acetic acid: water in a 50:8:42 ratio) and shaken with a vortex mixer for 1 minute. The sample was then centrifuged at 10,000 rpm for 5 min and filtered. The total phenolic content was analyzed using Folin-Ciocalteau colorimetry as described by [30]. Next, to determine the surface bioactive compounds, 0.1 g of KLE encapsulated powder was dissolved in

View Article Online
DOI: 10.1039/D5FB00648A

a mixed solution of ethanol and methanol (1:1 ratio) and shaken with a vortex mixer for 1 minute. The sample was filtered, and the total phenolic content was again analyzed using Folin-Ciocalteau colorimetry.

The encapsulation efficiency (%) was calculated using the following formula (Eq.2) according to [31]:

$$EE = [(T_o - S_o)/T_o]\, x100 \quad (2)$$

where T_O represents the total bioactive compounds, and S_O represents the surface bioactive compounds.

2.4. Determination of physical attributes of KLE microcapsules

2.4.1. Determination of moisture content and water activity

The moisture content of KLE microcapsules was measured using an infrared moisture analyzer (MA35, Sartorius, Goettingen, Germany) according to the method described by [32]. Additionally, the water activity (a_w) at 25°C was determined with an Aqua Lab instrument (AquaLab Pre, Decagon, QTEtech, Hanoi, Vietnam). The reported results are an average of three replicates.

2.4.2. Determination of color attributes

According to the method outlined by [32], the color of KLE microcapsules was measured using a portable spectrophotometer (CM-600d, Konica Minolta, INC, Osaka, Japan) within the Lab system. The color values were expressed using the CIE L*a*b* system, where the brightness coordinate L* indicates whiteness/darkness, the chromaticity coordinate a* indicates redness/greenness, and the chromaticity coordinate b* indicates yellowness/blueness. All measurements were taken in triplicate, and the mean values were recorded. The total color difference, ΔE, was subsequently calculated using the following formula (Eq. 3),

View Article Online
DOI: 10.1039/D5FB00648A

$$\Delta E = \sqrt{(L^*_i - L^*_t)^2 + (a^*_i - a^*_t)^2 + (b^*_i - b^*_t)^2} \quad (3)$$

where L^*_i, a^*_i, and b^*_i are the initial values for KLE microcapsules at zero days, and L^*_t, a^*_t, and b^*_t are the measured values at different storage times.

2.4.3. Determination of water solubility

The water solubility measurement was performed following the procedure outlined by [33] involved adding 1 g of KLE microcapsules to 100 mL of distilled water, and then the mixture was stirred utilizing a magnetic stirrer (SCILOGEX, model SCI550-S, USA) for 30 min. Afterward, the mixture was centrifuged (Centrifuge Kubota, series 6000, Japan) at 3000×g for 5 min. A 25 mL aliquot of the supernatant was transferred to a pre-weighed petri dish and dried in an oven (Memmert, DO 6062, Germany) operated at a temperature of 105°C for a period of 5 h (Aliquot homogenized before drying**)**. The solubility was estimated utilizing the following formula (Eq. (4)).

$$Water\ solubility(\%) = \frac{Solid\ content\ in\ supernatant}{Total\ solid\ content} \times 100 \quad (4)$$

2.5. Determination of phytochemicals properties of KLE microcapsules

2.5.1. Measurements of total phenolic content (TPC)

TPC of KLE microcapsules was measured using a modified approach based on [34]. Briefly, a 1 g of microencapsulated samples was added to 5 mL of distilled water, and then 0.5 mL of Folin–Ciocalteu phenol reagent was added. The mixture was incubated for 8 min, afterward, 1.5 mL of 20% Na_2CO_3 was added, and the mixture was left at 25 °C for 20 min (calibration: 0–200 mg GAE/L, R^2=0.994; samples diluted to 0.2–0.8 AU**)**. UV–vis Spectrophotometer (Eppendorf BioSpectrometer® basic, Thailand) was utilized to measure the absorbance of the sample at 765 nm, using a blank for reference, according to [27], Gallic acid was

View Article Online
DOI: 10.1039/D5FB00648A

used as the standard for the calibration curve (Y=4.83 X + 0.0792, R^2=0.994). TPC was expressed as gallic acid equivalents (mg GAE/mL). Three independent extractions and encapsulations were carried out in triplicate, with each replicate measured three times; data are presented as mean ± SD.

2.5.2. Analysis of total flavonoid content (TFC)

To assess TFC, 1 mL of the microencapsulated solution was added to 1 mL of 2% w/v aluminum chloride in methanol and incubated for 30 min. UV–vis Spectrophotometer (Eppendorf BioSpectrometer® basic, Thailand) was used to measure the absorbance at 430 nm using a with a blank for reference, using a cuvette spectrophotometer [35]. TFC (mg QE/mL) was calculated based on the quercetin calibration curve (Y=0.8986 X + 0.024, R^2 = 0.995). Three independent extractions and encapsulations were carried out in triplicate, with each replicate measured three times; data are presented as mean ± SD.

2.5.3. Determination of antioxidant activity by DPPH scavenging activity

Following a slightly modified version of the procedure used by [36, 37], the 2,2-Diphenyl-1-picrylhydrazyl (DPPH) assay was utilized to evaluate the antioxidant activity of KLE microcapsules. A 0.2 mL of aqueous extract (from 1 g powder in 10 mL water consistent with TPC extraction for comparability was added to 2 mL of methanol and 2 mL of the DPPH solution. The mixture was incubated for 30 min at 25 °C in the dark. Following incubation, UV–vis Spectrophotometer (Eppendorf BioSpectrometer® basic, Thailand), the absorbance was determined at 517 nm. Methanol served as the blank, and the values of antioxidant activity of KLE microcapsules were then computed using the specified equation (Eq. 5). Antioxidant activity was quantified against a Trolox calibration curve (0–1000 μM; R^2=0.993 for DPPH.

2.5.4. Determination of antioxidant activity by ferric reducing antioxidant power (FRAP)

View Article Online
DOI: 10.1039/D5FB00648A

To determine the FRAP antioxidant activity of KLE microcapsules, 1 g of KLE microcapsules was dissolved in 10 mL of distilled water and thoroughly mixed using a vortex mixer for 3 min. The sample was placed in a hot tub, maintaining a shaking temperature of 30℃ for up to 30 min. Next, the sample was subjected to centrifugation at 4000 rpm for 20 min [31]. Then, 2.85 mL of FRAP solution was mixed with 0.15 mL of the sample. The FRAP solution was prepared by combining acetate buffer (300 mM, pH=3.6), 20 mM $FeCl_3$, and TPTZ solution (40 mM HCl for TPTZ) in a ratio of 10:1:1 and warming it to 37.5℃ before use. After the sample and FRAP solution were thoroughly mixed, the mixture was incubated for 30 min. Antioxidant activity was quantified against a Trolox calibration curve (0–1000 µM; R^2=0.991 for FRAP. The absorbance was measured at 593 nm [38]. The DPPH and FRAP inhibition were calculated using the following formula (Eq. 5):

$$\% \text{ Inhibition} = \left[1 - \frac{A_{sample}}{A_{control}}\right] x\ 100 \quad (5)$$

Where $A_{control}$ denotes the mixture of methanol and DPPH solution, and A_{sample} refers to the mixture of the extract and DPPH / FRAP solution.

2.5.5. Determination of total tannin content (TTC)

The tannin content in KLE microcapsules was assessed using a method adapted from [39]. In summary, 500 µL of extract (from 0.1 g of KLE microcapsules in 1 mL water) were incubated with 10 mg polyvinylpolypyrrolidone (PVPP) (to bind tannins) or without (replaced by water as control) for 15 min at 4°C, followed by centrifugation at 15,000× g for 10 min. The supernatants were then analysed using the total phenolic content (TPC) assay. The tannin content was calculated based on the difference in TPC values between the PVPP-treated and water-treated samples. Tannic acid (0–100 µg/mL) served as the standard, and tannin levels were reported as mg TAE/100 mL.

View Article Online
DOI: 10.1039/D5FB00648A

2.5.6. Mitragynine quantification by HPLC

Mitragynine content in KLE microcapsules was quantified using high-performance liquid chromatography (HPLC) with UV detection. Approximately 100 mg of encapsulated powder was extracted with 10 mL of methanol containing 0.1% formic acid, vortexed for 1 min, sonicated for 15 min at ambient temperature, and centrifuged (5000 g, 10 min). The supernatant was diluted as needed, filtered through a 0.22 µm PTFE syringe filter, and transferred to vials. Chromatographic analysis was performed on a C18 column (150 × 4.6 mm, 5 µm; 35 °C) using a binary gradient system consisting of water with 0.1% formic acid (solvent A) and acetonitrile with 0.1% formic acid (solvent B). The gradient program was: 35% B (0 min) → 55% B (6 min) → 70% B (10 min, held to 12 min) → 35% B (12.1 min, re-equilibrated to 20 min). The flow rate was 1.0 mL min^{-1}, injection volume 10 µL, and detection wavelength 225 nm. Calibration curves were prepared using mitragynine standard solutions (0.05–50 µg/mL), yielding linearity with $r^2 \geq 0.999$. Method performance was validated with a limit of quantification (LOQ) of 0.05 µg/mL, precision (RSD) ≤ 5%, and recovery of 90–110% from spiked matrix samples. Mitragynine concentrations were expressed as mg/g dry basis, corrected for residual moisture.

2.6. Assessment of morphology of KLE microcapsules

To assess the microstructure of KLE microcapsules, the appearance of the microcapsules was examined using a scanning electron microscope (SEM) and an energy dispersive X-ray spectrometer (JEOL, JSM-IT300 Oxford, X-Max N 20) with a 15 kV magnification at 1000×, 3000×, 5000×**.** Samples were sputter-coated with gold (10 nm thickness) under vacuum before imaging.

2.7. Investigation of storage stability of KLE microcapsules

View Article Online
DOI: 10.1039/D5FB00648A

Formulations were selected using a multi-criteria optimization approach that considered lowest MC/aw and highest TPC, TFC, and antioxidant activity**.** Weighted scoring was applied **(**40**%** bioactive retention, 30**%** physical stability, 30**%** solubility**)**, with the GA@160 °C formulation achieving the highest score **(**85/100**).** Ten grams of KLE microcapsules, encapsulated using gum Arabic and processed via spray drying at 160°C, were packaged in laminated aluminum foil bags and stored under vacuum conditions at room temperature (30±5°C). Quality properties were monitored every 15 days over a period of 90 days to assess changes.

2.8. Kinetics modelling of changes in characteristics of KLE microcapsules

To estimate the reaction order of the alterations in various characteristics of KLE microcapsules, the experimental data were analysed using Eq**.** 6. Zero-order and first- order equations, which are frequently employed to model reactions associated with food quality deterioration, were derived from Eq.6 and are represented in Eqs. 7-8.

$$-\frac{dC}{dt} = kC^n \quad (6)$$

$$C = C_o \pm k\,t \quad (7)$$

$$lnC = lnC_o \pm k\,t \quad (8)$$

In the given equations, C and C_o denote the property value at a specific time and the initial value, respectively, while "t" indicates the storage duration. The parameter "k" is the reaction rate constant (day^{-1}), and "n" represents the reaction order of the changes. The symbols (+) and (-) indicate the increase and decrease in attributes, respectively.

2.9. Predicting the shelf life by integration of the quality properties

View Article Online
DOI: 10.1039/D5FB00648A

Shelf-life was estimated based on the minimum time to first failure among key physicochemical and phytochemical attributes, namely moisture content (MC), water activity (aw), total phenolic content (TPC), total flavonoid content (TFC), total tannin content (TTC), antioxidant activity by DPPH radical scavenging, and ferric reducing antioxidant power (FRAP).

For each parameter, a threshold value was defined to indicate the point of quality loss. Specifically, the water activity threshold was set at 0.30, as values above this level promote chemical reactions and increase the risk of microbial growth [40, 41]. For antioxidant stability, shelf-life termination was determined when DPPH radical scavenging activity decreased by 20% relative to the initial value, which was considered a critical limit for functional quality retention.

A least-squares fitting procedure was employed to ascertain the kinetic orders by adjusting the experimental data to solve the general expression of Eq. 6. The kinetic parameters derived for each attribute were then used to estimate the shelf life of KLE microcapsules using Eq. 9, as demonstrated in prior studies by [16].

$$Shelf\ life\ (day) = \frac{C - C_0}{k} \qquad (9)$$

2.10. Data Analysis

Data were analyzed using two-way analysis of variance (ANOVA) to evaluate the effects of wall material and drying temperature on the on the properties of KLE microcapsules, and mean comparisons were performed using Tukey's HSD test at a significance level of $p < 0.05$. Significant differences among wall materials are denoted by uppercase letters, while differences among temperatures are indicated by lowercase letters. Effect size was also computed to investigate the importance of each factor. Moreover ,regression analysis was performed to evaluate the precision of the models in representing the observed data. The selection of the best model was based on achieving the highest correlation coefficient, $R^2 \geq 0.90$, as recommended by

View Article Online
DOI: 10.1039/D5FB00648A

previous studies [42]. Data analysis and modelling were carried out using Minitab v. 18 (Minitab Inc., State College, PA, USA). The proportion of variance explained by each factor was expressed as eta-squared (η^2) values obtained from the ANOVA, indicating the relative effect size of wall material, inlet temperature, and their interaction.

3. Results and Discussion

3.1 Encapsulation Yield of KLE Microcapsules

The two-way ANOVA results revealed significant main and interaction effects of wall material and temperature on encapsulation yield. The encapsulation yield ranged from 58.2 to 72.9%, with wall material exerting a moderate effect ($\eta^2 = 0.28$). Resistant maltodextrin (RM) generally produced higher recovery values compared to gum Arabic (GA), underscoring the importance of carrier selection in determining encapsulation efficiency. In contrast, temperature exhibited only a small effect ($\eta^2 = 0.07$), suggesting that drying conditions had a limited influence on yield relative to wall material composition, as illustrated in Table 2. Higher excipient concentrations in RMD and blend experiments contributed to reduced wall adhesion, enhancing yield. The low yield for gum Arabic is attributed to its pseudoplastic nature at high concentrations (20% in this study), which increases viscosity [43] and causes it to adhere to the inner surfaces of the spray dryer, reducing yield. Additionally, increasing the spray drying temperature from 150°C to 160°C significantly ($p \leq 0.05$) improved the yield when using gum Arabic as the coating material. Higher temperatures enhance thermal energy, breaking intermolecular bonds, which reduces viscosity and adhesion to the spray dryer surfaces [44].

Conversely, using resistant maltodextrin alone or in combination with gum Arabic resulted in lower yields at higher spray drying temperatures. This is likely due to heat

View Article Online
DOI: 10.1039/D5FB00648A

accumulation causing the microcapsules to melt and stick to the inner surfaces of the spray dryer, thereby decreasing the overall yield.

3.2 Encapsulation Efficiency of KLE Microcapsules

The results presented in Table 2, revealed that the values of encapsulation efficiency (EE), ranged from 68.3% to 92.7%, with both wall material and temperature exerting strong influences (η^2 = 0.32 and 0.18, respectively), alongside a significant interaction effect (η^2 = 0.11). Similarly, hygroscopicity (HG), which varied between 7.2% and 12.5%, was markedly influenced by wall material (η^2 = 0.26) and temperature (η^2 = 0.14), with an additional moderate interaction (η^2 = 0.09). The use of gum Arabic as a coating material at an inlet spray drying temperature of 160°C resulted in the highest encapsulation efficiency, while resistant maltodextrin at the same temperature resulted in the lowest efficiency. Gum Arabic's emulsion properties enable it to form a better encapsulating film compared to resistant maltodextrin, leading to higher encapsulation efficiency for microcapsules coated with gum Arabic [45].

Considering the inlet spray drying temperature, higher temperatures led to more effective water evaporation from the particles, thus increasing encapsulation efficiency. However, excessively high temperatures might damage the microcapsules, exposing the core material to direct heat and potentially degrading the active compounds [46]. Consequently, microcapsules using maltodextrin and a combination of resistant maltodextrin with gum Arabic exhibited reduced encapsulation efficiency when the inlet spray drying temperature increased to 160°C. In general, Encapsulation efficiency values were benchmarked against the initial TPC in the crude extract (45.2 ± 2.1 mg GAE/mL), indicating 82–92% retention post-encapsulation and thereby confirming effective protection.

3.3 Moisture Content (%) and water activity (a_w) of KLM microcapsules

View Article Online
DOI: 10.1039/D5FB00648A

The study examined the moisture content and water activity of KLM microcapsules produced through spray drying, varying the types of coating materials and two inlet drying temperatures (Table 2). Moisture content ranged from 2.6 to 6.8%, being more strongly affected by temperature ($\eta^2 = 0.27$) than wall material ($\eta^2 = 0.15$). Higher inlet temperature reduced moisture in GA samples but slightly increased it in RM powders, suggesting carrier-dependent responses to drying kinetics. It was found that microcapsules with gum Arabic as the coating material had higher moisture content compared to those using resistant maltodextrin. This is because gum Arabic, a complex heteropolysaccharide, is hydrophilic, enabling it to retain more moisture than resistant maltodextrin. Water activity or moisture content below Tg **(**~50°C for GA/RMD**)**, ensures glassy state stability [47]**.**

When the inlet spray drying temperature was increased from 150°C to 160°C, the moisture content of microcapsules with gum Arabic decreased, as the higher temperature facilitated better water evaporation [48]. GA exhibits higher viscosity at lower temperatures, which can trap moisture; at elevated temperatures, viscosity decreases, facilitating evaporation. In contrast, RMD is inherently less viscous and less affected by this behavior. In contrast, microcapsules with resistant maltodextrin and those with a combination of gum Arabic and resistant maltodextrin showed an increase in moisture content (3.52 ±0.1% and 3.34±0.2%, respectively) at higher temperatures (Table 2). Higher temperatures generate a steeper heat gradient, enhancing moisture diffusion in RMD but leading to tackiness in the blends (Tay et al., 2021).

Clearly from Table 2, water activity (a_w) values were low (0.16–0.26), suitable for storage stability. Both factors had small effects ($\eta^2 \leq 0.12$), indicating robustness across treatments., which are within the standard reference values for food powders that should not

View Article Online
DOI: 10.1039/D5FB00648A

exceed a water activity of 0.3. Water activity (a_w) is more closely associated with bound water; GA's hydrophilic nature tightly binds water, which maintains low a_w values even at higher total moisture content [49].

3.4 Water solubility *of KLE Microcapsules*

Water solubility was consistently high (91.8–95.6%), with significant though smaller effects of carrier ($\eta^2 = 0.22$) and temperature ($\eta^2 = 0.10$). Higher temperatures improved solubility slightly, likely through reduced moisture and better particle formation (Table 2), with the highest solubility observed in microcapsules coated with resistant maltodextrin (95.8±0.09%). The branched structure of resistant maltodextrin enhances its density, and the presence of hydroxyl groups allows it to bond with water molecules effectively, resulting in superior solubility compared to those coated with gum Arabic or a combination of both [50]. In addition, higher temperatures reduce residual moisture, enhancing particle dispersibility; low MC minimizes clumping upon reconstitution**.**

The large, porous amorphous structure of the microcapsules using resistant maltodextrin as a coating material facilitates easy dissolution in water, aligning with the findings of Jordan et al. (2018), which indicated that resistant maltodextrin-coated microcapsules have better solubility than those coated with gum Arabic. Additionally, increasing the inlet drying temperature from 150°C to 160°C improved the water solubility of microcapsules coated with gum Arabic and the combination of gum Arabic and resistant maltodextrin. The higher drying temperature reduces moisture content, thereby enhancing the ability of the microcapsules to dissolve in water. In other words, tackiness affects internal evaporation but not external solubility; lower moisture content from optimal temperatures aids dissolution**.** This is consistent

View Article Online
DOI: 10.1039/D5FB00648A

with the research of Astina & Sapwarobol **(**2019**)**, which showed that lower moisture content improves the solubility of powdered milk.

3.5 Color parameters (L* a* b*) of KLE microcapsules

Color attributes (L*, a*, b*) showed meaningful changes as indicated in Table 2. Lightness (L*; 60.4–64.8) was moderately influenced by both carrier ($\eta^2 = 0.19$) and temperature ($\eta^2 = 0.14$). The a* values (–1.29 to –0.44) showed a strong wall material effect ($\eta^2 = 0.24$), reflecting GA's tendency toward less negative redness–greenness. The b* values (4.1–8.3) showed the strongest carrier effect ($\eta^2 = 0.32$), confirming the distinct visual profiles imparted by GA

The L* value, which ranges from 0 (dark) to 100 (light), showed that microcapsules coated with resistant maltodextrin were lighter than those coated with gum Arabic or a combination of both. This is because resistant maltodextrin is a white powder, resulting in a bright white color when dissolved in water, whereas gum Arabic is a light-yellow powder that turns brown when dissolved. Therefore, microcapsules with resistant maltodextrin as the coating material appeared lighter than those with gum Arabic. The inlet drying temperature did not significantly affect the L* value of the microcapsules ($p \leq 0.05$).

The a* value indicates the red-green spectrum, with negative values representing green and positive values representing red. Similarly, the b* value indicates the yellow-blue spectrum, with positive values representing yellow. An increase in the inlet drying temperature from 150°C to 160°C resulted in higher b* values for KLE microcapsules. This is attributed to the Maillard reaction, which intensifies yellow coloration at higher temperatures [51].

3.6 Phytochemical properties of KLE microcapsules

3.6.1 Total Phenolic Compounds

View Article Online
DOI: 10.1039/D5FB00648A

From Table (2), It was observed that total phenolic content (TPC) ranged from 13.1 to 34.8 mg GAE/mL and was strongly influenced by wall material ($\eta^2 = 0.29$), with GA promoting higher retention. Temperature contributed moderately ($\eta^2 = 0.16$), suggesting heat-stimulated release or degradation depending on carrier type. When considering the impact of temperature, increasing the inlet temperature from 150°C to 160°C resulted in a higher total phenolic content in the microcapsules. The higher temperature facilitated faster drying and the formation of a protective film layer around the microcapsules, which shortens the exposure time of the phenolic compounds to heat. Additionally, higher drying temperatures may possibly induce faster film formation and polymerization reactions that could lead to an increase in the total phenolic content [52].

Regarding the coating material, microcapsules coated with gum Arabic demonstrated a higher total phenolic content compared to those coated with resistant maltodextrin or a combination of resistant maltodextrin and gum Arabic. This is because gum Arabic has emulsifying properties that enhance stability and can form a well-structured polymer film around the microcapsules [53].

3.6.2 Total Flavonoid Content

The results shown in Table 2 revealed that total flavonoid content (TFC) varied between 1.8 and 5.1 mg QE/mL. Carrier was again dominant ($\eta^2 = 0.30$), with GA-based formulations consistently higher. Specifically, microcapsules coated with gum Arabic exhibited the highest total flavonoid content. This is due to the matrix formation between the gum Arabic coating and the core substance, which helps reduce the loss of total flavonoid content. Additionally, the emulsifying properties of gum Arabic enhance stability and protect the active compounds from environmental conditions [54].

View Article Online
DOI: 10.1039/D5FB00648A

In contrast, the inlet temperature during spray drying (150°C and 160°C) did not significantly affect the total flavonoid content. Increasing the inlet temperature from 150°C to 160°C did not significantly impact the total flavonoid content ($p>0.05$). Flavonoids may be more heat-stable or better protected by matrix; TPC includes broader reducing species sensitive to heat**.** The microcapsules coated with gum Arabic had the highest total flavonoid content at both 150°C and 160°C (4.98 ± 0.8 and 5.22 ± 0.12 mg QE/mL db., respectively), followed by those coated with resistant maltodextrin combined with gum Arabic (3.08 ± 0.23 and 2.99 ± 0.35 mg QE/mL db., respectively), and finally those coated solely with resistant maltodextrin (1.67 ± 0.5 and 1.61 ± 0.72 mg QE/mL db., respectively).

3.6.3 Antioxidant activity using the DPPH assay

The results revealed that antioxidant activity showed strong wall material effects. DPPH scavenging activity ranged from 233.5 to 305.2 μmol TE/100 mL ($\eta^2 = 0.27$), as it can be seen in Table 2. GA preserved and even enhanced antioxidant activity compared to RM.

Increasing the inlet temperature during spray drying resulted in a corresponding increase in antioxidant activity, which can be explained by the higher drying temperature enhancing the antioxidant properties of the microcapsules [47]. This trend is attributed to the direct correlation between antioxidant activity and phenolic compound content; higher levels of phenolic compounds generally lead to increased antioxidant activity [55].

3.6.4 Antioxidant activity using the FRAP assay

As it can be observed from Table (2), the results indicated that FRAP varied more broadly (317.5–522.7 μmol TE/100 mL), with carrier ($\eta^2 = 0.33$) and temperature ($\eta^2 = 0.21$) both important. GA preserved and even enhanced antioxidant activity compared to RM.

View Article Online
DOI: 10.1039/D5FB00648A

When examining the type of coating material, microcapsules coated with gum Arabic and those coated with a combination of resistant maltodextrin and gum Arabic showed no significant statistical difference in FRAP antioxidant activity. However, gum Arabic-coated microcapsules demonstrated higher antioxidant activity compared to those coated with resistant maltodextrin. This is because the film layer formed by gum Arabic better prevents oxidation reactions compared to resistant maltodextrin [56]

Regarding the temperature factor, increasing the inlet temperature in the spray drying process from 150°C to 160°C resulted in a significant change in FRAP antioxidant activity ($p \leq 0.05$). This could be attributed to the higher inlet temperature causing microcapsule particles to crack, which leads to direct exposure of antioxidants to heat and subsequent loss due to direct heat exposure [57].

3.6.5 Total Tannin Content

The results presented in Table 2 revealed that total tannin content (TTC) followed a similar trend (13.4–35.5 mg CE/mL), with both carrier ($\eta^2 = 0.25$) and temperature ($\eta^2 = 0.20$) exerting effects, highlighting synergistic contributions. It was found that both the type of coating material and the inlet temperature during spray drying at 150°C and 160°C significantly affect the total tannin content. Specifically, microcapsules coated with gum Arabic and processed at an inlet temperature of 160°C exhibited the highest total tannin content (36.42 ±2.45 mg TAE/mL).

Increasing the inlet temperature from 150°C to 160°C resulted in a higher total tannin content in the microcapsules. This is because the higher temperature facilitates the formation of a well-structured film layer on the particle walls, which enhances the retention of tannins. Regarding the coating material, microcapsules using gum Arabic as the coating material demonstrated a higher total tannin content compared to those coated with resistant maltodextrin

View Article Online
DOI: 10.1039/D5FB00648A

or a combination of resistant maltodextrin and gum Arabic. This is due to gum Arabic's emulsifying properties, which improve stability and enable the formation of a polymer film around the microcapsules, similar to its effect on total phenolic content [53].

3.6.6. Mitragynine Stability

The chromatographic profile of kratom leaf extract (KLE), as revealed by HPLC analysis, demonstrated a distinct and well-resolved peak at approximately 6.9 min, corresponding to mitragynine (Figure 2). This identification was confirmed through comparison with an authentic standard, consistent with previous reports that place mitragynine's retention time between 6.5 and 7.0 min under reversed-phase conditions [58, 59]. The sharp symmetry and high intensity of this peak affirm mitragynine's predominance among the alkaloids present in KLE. Additional minor peaks observed between 2–5 min and 7–10 min likely represent polar phenolic compounds and structurally related alkaloids such as paynantheine and speciogynine.

The developed HPLC method exhibited a stable baseline and absence of interfering signals beyond 10 min, indicating high selectivity and robustness. These attributes are essential for reliable quantification of mitragynine in complex plant matrices and support the method's suitability for routine analysis in quality control and formulation studies.

Encapsulation studies further revealed that the retention of mitragynine in spray-dried microcapsules was significantly influenced by the choice of wall material. Gum Arabic (GA) consistently yielded the highest mitragynine content (1.89–1.96 mg/mL), outperforming resistant maltodextrin (RMD) and the RMD–GA blend. This superior performance is attributed to GA's highly branched polysaccharide structure and emulsifying properties, which enhance molecular entrapment and protect bioactives from thermal and oxidative degradation during spray drying [60, 61]. In contrast, RMD, while beneficial for moisture reduction and solubility, demonstrated lower

View Article Online
DOI: 10.1039/D5FB00648A

encapsulation efficiency for hydrophobic alkaloids like mitragynine, likely due to its limited molecular affinity [62].

Interestingly, inlet temperature (150 vs. 160 °C) did not significantly affect mitragynine retention across formulations, suggesting that wall material composition exerts a more dominant influence than thermal stress. This observation aligns with previous findings that emphasize the role of carrier–core interactions over processing temperature in determining encapsulation outcomes (Díaz-Montes, 2023).

Moreover, the retention trends of mitragynine paralleled those of total phenolic content (TPC) and antioxidant capacity (DPPH, FRAP), reinforcing the protective role of GA in preserving multiple classes of bioactives. The co-stabilization of alkaloids and phenolics is particularly relevant for the development of functional food and nutraceutical products, where both pharmacological efficacy and antioxidant potential are desired [60].

Collectively, these findings underscore the importance of wall material selection in microencapsulation strategies for botanical extracts. Gum Arabic, particularly at an inlet temperature of 160 °C, offers a promising formulation for preserving mitragynine and related bioactives, thereby enhancing the stability and functionality of KLE-based products.

3.7 Surface structure of KLE microcapsules analyzed by scanning electron microscopy (SEM)

The shape and structure of KLE microcapsules are influenced by various production factors, including the type of coating material, coating concentration, coating-to-liquid ratio, solution viscosity, inlet temperature of the spray dryer, and the flow rate of the solution through the spray dryer. These factors not only affect the visual appearance of the microcapsules but also impact the stability of the bioactive compounds within them. Smoother morphology in GA

View Article Online
DOI: 10.1039/D5FB00648A

correlates with higher bioactive retention via reduced surface exposure**.** Issues such as cracks or surface ruptures can decrease encapsulation efficiency and allow moisture infiltration, potentially leading to oxidation of the active compounds [63, 64].

Figure (3a) illustrates the morphology of microcapsules coated with resistant maltodextrin at an inlet temperature of 150°C. Analyzed using scanning electron microscopy (SEM) at magnifications of 1,000x, 3,000x, and 5,000x, these microcapsules generally appear spherical with relatively smooth surfaces and minor folds and dents, indicating effective encapsulation. Some particles tend to cluster slightly, which may be due to residual moisture in the coating material or moisture absorbed from the environment [65].

The morphology of microcapsules coated with gum Arabic at 150°C is shown in Figure (3b). These particles are typically smaller and exhibit more surface folds and dents compared to those coated with resistant maltodextrin. The increased surface irregularities are attributed to the rapid formation of the coating during the initial stage, leading to the swift evaporation of water within the particles [66].

Figure (3c) also depicts microcapsules coated with a 1:1 ratio of resistant maltodextrin and gum Arabic at 150°C. These capsules are mostly spherical with a mix of large and small particles. They show a tendency to be well-distributed without significant clustering but exhibit more surface folds and dents compared to capsules coated solely with resistant maltodextrin. This morphology is influenced by factors such as direct exposure to heat and rapid evaporation of water within the particles, leading to deformation and folds [65].

At a higher inlet temperature of 160°C, Figure (4a) shows microcapsules coated with resistant maltodextrin. The particles are mostly spherical with larger sizes and some smaller particles clumped together. The surface exhibits wrinkles and is partially smooth. In contrast,

View Article Online
DOI: 10.1039/D5FB00648A

Figure (4b) presents microcapsules coated with gum Arabic, which are generally smaller with a rough surface and significant wrinkling and crumpling. Figure (4c) depicts microcapsules coated with a 1:1 ratio of resistant maltodextrin and gum Arabic. These particles are small with a rough surface, showing pronounced crumpling and indentations compared to single coatings.

These observations highlight how different coating materials and inlet temperatures affect the structural characteristics of microcapsules. Higher temperatures and certain coating combinations can result in increased surface roughness and crumpling, which impacts the integrity and performance of the microcapsules [67].

3.8. Quality changes of KLE microcapsules during storage

3.8.1 Changes in physical properties of KLE microcapsules during storage

Figures (5a-b) show the moisture content and water activity of the KLE microcapsules, respectively. The initial moisture content of the KLE microcapsules was 2.65±0.1%. Over time, the moisture content increased to 2.75±0.2%, 2.85±0.25%, 2.94±0.15%, 3.05±0.2%, 3.22±0.1%, and 3.33±0.16% after 15, 30, 45, 60, 75, and 90 days of storage, respectively. The initial water activity of the KLE microcapsules was 0.164±0.03. With prolonged storage, the water activity increased to 0.193±0.07, 0.221±0.04, 0.243±0.01, 0.256±0.04, 0.289±0.07, and 0.317±0.03 after 15, 30, 45, 60, 75, and 90 days, respectively.

The moisture content and free water of the KLE microcapsules did not exceed the spoilage indicators set (moisture content ≤ 5% and water activity < 0.6) even after 90 days of storage. This is due to the aluminum foil packaging's excellent ability to prevent moisture and water vapor from the air [68]. The aluminum foil has a water vapor and oxygen permeability of only water vapor transmission rate of 0.06571 g/m²/day and oxygen transmission rate of 0.00873 mL/m²/day, respectively [69]. This low permeability explains why the aluminum foil

View Article Online
DOI: 10.1039/D5FB00648A

packaging minimizes water and oxygen absorption under vacuum conditions, resulting in only a slight increase in moisture and free water content. Water activity can serve as an indicator of product stability against oxidation reactions, such as fat oxidation and rancidity. A water activity of less than 0.6 indicates that the sample remains stable or has good shelf stability [70]. These results are consistent with [71], who studied the storage of papaya powder in aluminum foil bags and found that the water activity of the papaya powder remained below 0.6 after 7 weeks of storage.

The progressive increase in total color difference (ΔE) observed in spray-dried KLE encapsulates over the 90-day storage period reflects gradual pigment degradation and structural changes within the microcapsules. Initially, the ΔE value was 0 on day 0, indicating no perceptible color change. A marked increase to ΔE = 0.40 by day 15 suggests an early phase of rapid color modification. This may be attributed to residual moisture and initial oxidative reactions, which are known to affect polyphenolic compounds and sensitive pigments [72].

Following this initial phase, the rate of color change decelerated, with ΔE values reaching 0.44 and 0.46 on days 30 and 45, respectively. This plateau-like behavior implies that the encapsulated system may have achieved a degree of equilibrium in pigment stability and wall matrix integrity, thereby reducing the rate of further degradation. Similar stabilization trends have been reported in encapsulated anthocyanins and carotenoids, where wall materials such as maltodextrin and gum Arabic mitigate oxidative stress and thermal instability [73].

Between days 60 and 90, ΔE values continued to rise gradually from 0.51 to 0.58, indicating ongoing but limited degradation. This phase likely involves slower oxidative processes and potential Maillard-type reactions, which are common during prolonged storage of encapsulated bioactives [74]. Importantly, the final ΔE value remained below 1.0, a threshold

View Article Online
DOI: 10.1039/D5FB00648A

generally considered imperceptible or only slightly noticeable to the human eye. This suggests that the encapsulation matrix provided effective protection against color deterioration, preserving the visual quality of the product.

Overall, these findings demonstrate that the selected encapsulation strategy offers substantial color stability over time. The minor perceptible changes observed after three months of storage underscore the efficacy of the wall materials in limiting oxidative and thermal degradation of sensitive compounds. This stability is critical for maintaining both the aesthetic and functional attributes of KLE encapsulates, particularly in applications where visual appeal and bioactive retention are essential.

3.8.3 Changes in total phenolic compounds during storage

Figure (6a) shows the decrease in total phenolic compounds in KLE microcapsules during storage. Initially, the total phenolic content of the microcapsules was 36.78 ± 3.08 mg GAE/mL. Over time, this amount gradually decreased, with total phenolic compounds measuring 34.83 ± 1.52, 33.20 ± 0.65, 32.66 ± 1.04, 31.88 ± 0.67, 30.36 ± 0.89, and 30.10 ± 0.45 mg GAE/mL. at 15, 30, 45, 60, 75, and 90 days of storage, respectively. Several factors can lead to the reduction in total phenolic compounds, including temperature, increased moisture, and the amount of air permeating the packaging and coming into contact with the product [75]. These results align with research by [76], which found a reduction in phenolic content in ground coffee stored in aluminum foil bags.

3.8.4 Changes in total flavonoid contents during storage

Figure (6b) displays the decrease in total flavonoids in KLE microcapsules during storage. The initial total flavonoid content was 5.22 ± 0.12 mg QE/mL. This amount gradually decreased over time, with values of 5.15 ± 0.15, 4.95 ± 0.09, 4.85 ± 0.23, 4.75 ± 0.12, 4.54 ±

View Article Online
DOI: 10.1039/D5FB00648A

0.15, and 4.32 ± 0.05 mg QE/mL. at 15, 30, 45, 60, 75, and 90 days of storage, respectively. Key factors affecting the total flavonoid content include temperature, light, and oxygen. The primary cause of the decrease in flavonoid content is oxidation during storage, a common reaction in food preservation. This hypothesis aligns with the research of [77], which studied the stability of bioactive compounds in rowan berries. Their study found that flavonoid levels in berries decreased by up to 86% during 20 weeks of storage. Therefore, oxidation directly impacts the reduction in flavonoid content. Similarly, [78] examined the impact of packaging material on the quality of powdered milk over 12 months. They found that powdered milk packaged in aluminum foil experienced a lower reduction in flavonoids compared to other packaging materials, as aluminum foil blocks light and has low moisture and oxygen permeability. This indicates that packaging material directly affects the reduction in total flavonoid content in KLE microcapsules.

3.8.5 Changes in total tannins during storage

Figure (6c) illustrates the decrease in total tannins in KLE microcapsules during storage. The initial total tannin content was 36.42 ± 2.45 mg TAE/mL. Over time, this amount gradually decreased, with total tannins measuring 33.83 ± 1.25, 32.20 ± 1.56, 31.66 ± 1.05, 30.75 ± 0.85, 29.29 ± 0.45, and 29.08 ± 0.06 mg TAE/mL. at 15, 30, 45, 60, 75, and 90 days of storage, respectively. This trend mirrors the decrease observed in total phenolic compounds and total flavonoids, which also decreased with extended storage time. These findings are consistent with research by [79], which investigated tannin extraction from kluwek fruit and its stability. Their study found that tannin extracted from kluwek fruit and stored in opaque glass containers had a shelf life of about 15 days, while tannins exposed to air and light had a shelf life of only 9 h. The darker color of kluwek fruit extracts may result from direct light exposure, which increases light

View Article Online
DOI: 10.1039/D5FB00648A

absorption and accelerates oxidation reactions that can degrade tannins [80]. Thus, packaging, light, and temperature are crucial factors affecting the stability and shelf life of KLE microcapsules.

3.8.6 Changes in antioxidant activity (DPPH) and antioxidant activity (FRAP) during storage

Figure 7a illustrates the reduction in antioxidant activity of KLE microcapsules as measured by the DPPH method during storage. Initially, the antioxidant activity was 293.55 ± 3.28 μM TE/100 mL. This value gradually decreased over time, reaching 283.06 ± 5.76, 271.45 ± 4.32, 265.53 ± 2.15, 258.06 ± 3.52, 247.65 ± 2.85, and 227.88 ± 4.64 μM TE/100 mL. at 15, 30, 45, 60, 75, and 90 days, respectively. This trend is consistent with the decrease in total phenolic compounds, as phenolics are directly related to antioxidant activity [81]. A study by [78] on the antioxidant activity of commercial powdered milk using the DPPH method found a 42.37% reduction in antioxidant activity over one year of storage. Their results indicated that packaging material significantly affects the reduction in antioxidant activity.

Similarly, antioxidant activity measured by the FRAP method also showed a decline over time (Figure 7b). The FRAP values for the KLE microcapsules were 522.74 ± 2.47, 477.49 ± 3.56, 469.32 ± 3.12, 459.35 ± 2.76, 435.56 ± 5.62, 422.63 ± 2.89, and 409.67 ± 8.51 μM TE/100 mL at days 1, 15, 30, 45, 60, 75, and 90, respectively. The observed reduction in antioxidant activity during storage indicates that antioxidant capacity decreases with prolonged storage time, and packaging material plays a crucial role in preserving the antioxidant activity of KLE microcapsules.

View Article Online
DOI: 10.1039/D5FB00648A

3.9. Kinetic modelling of changes in the properties of KLE microcapsules over storage period

In food science, kinetic modelling is a widely used technique to understand the changes in quality that occur during food processing. To characterize the changes in attributes (a_w, MC, TPC, TFC, TTC, DPPH, and FRAP) of KLE microcapsules over time, experimental data for these properties were fitted to proposed models using regression analysis. Figures (5-7) provide graphical representations of the zero-order and first-order equations that describe the changes in these properties during storage. The estimated kinetic parameters for the models were determined using regression analysis technique and listed in Table 3.

Generally, R^2 values of both zero-order and first-order were greater than 0.95, indicating that both models effectively describe the degradation kinetics of the studied properties, with first-order models generally providing a slightly better fit for most properties. Previous studies have reported that both zero-order and first-order models effectively described the alterations in the quality properties over the storage period of the studied materials [82-84]

3.10. Prediction of shelf life of KLE microcapsules

The period during which a product maintains its satisfactory quality before deteriorating is known as its shelf life [16]. During storage, quality changes occur, leading to degradation that may limit the product's shelf life. By incorporating the reaction rate constants obtained from kinetic modelling of quality attribute changes (Eq. 6) into Eq. 9, it is possible to predict the shelf life of KLE microcapsules. This equation allows for shelf-life prediction based on key quality determinants such as a_w, MC, TPC, TFC, TTC, DPPH, and FRAP. Based on minimum moisture content and water activity, the predicted shelf-life values are detailed in Table 3. The shelf lives

View Article Online
DOI: 10.1039/D5FB00648A

for the various properties of KLE microcapsules range from approximately 81 to 99 days, indicating their potential stability and longevity under the studied conditions.

4. Conclusions

This study demonstrated that spray drying offers a sustainable and scalable technique for producing kratom leaf extract (KLE) microcapsules with enhanced stability and bioactive retention. By utilizing plant-based, biodegradable wall materials—resistant maltodextrin and gum Arabic—the process aligns with environmentally conscious food formulation practices. Results showed that resistant maltodextrin yielded the highest encapsulation yield and solubility, while gum Arabic at 160°C provided superior antioxidant retention, phenolic and flavonoid content, and encapsulation efficiency. Gum Arabic, particularly at an inlet temperature of 160 °C, offers a promising formulation for preserving mitragynine and related bioactives, thereby enhancing the stability and functionality of KLE-based products. Despite slight differences in moisture content, both encapsulants maintained acceptable water activity, contributing to shelf-life stability. The application of kinetic models further allowed prediction of microcapsule degradation during storage, with estimated shelf lives ranging from 81 to 99 days.

However, it should be noted that unequal wall-solid concentrations across carriers (20% GA vs. 40% RMD) may have influenced atomization, viscosity, and yield outcomes, thereby limiting the strength of direct comparisons. Future studies should validate these findings under isosolid feed conditions to ensure robust comparisons across encapsulants. Moreover, while spray drying presents promise as a practical and environmentally aligned encapsulation method, energy consumption data were not collected in this study; thus, no claims regarding “low-energy processing” can be made at this stage.

View Article Online
DOI: 10.1039/D5FB00648A

These findings support the development of sustainable functional food systems by minimizing degradation, reducing food waste, and encouraging the use of renewable, low-impact ingredients in clean-label product design.

Credit Author Statement

Supanit Khongtongsang: Investigation, Formal analysis, Data curation and Writing – original draft. Mohammed Fikry: Investigation, Formal analysis, Data curation and Writing – original draft. Saeid Jafari: Data curation and Writing – original draft. Sochannet Chheng: Data curation and Writing – original draft. Isaya Kijpatanasilp: Data curation and Writing – original draft. Kitipong Assatarakul: Conceptualization, Data curation, Funding acquisition, Project administration, Supervision, Writing – original draft and Writing – review & editing.

Declaration of Competing Interest

Authors have no conflict of interest

Data availability

The data supporting the findings of this study are available from the corresponding author upon request.

Funding

This study was funded by the 90th Anniversary of Chulalongkorn University Scholarship through the Ratchadapisek Somphot Endowment Fund (Grant no. GCUGR1125671051M), awarded to Supanit Khongtongsang.

View Article Online
DOI: 10.1039/D5FB00648A

References

1. W. F. Dewatisari and E. Nuryandani, *In Proceeding International Seminar of Science and Technology*, 2025, **4**, 49-62.
2. S. Charoenratana, C. Anukul and A. Aramrattana, *International Journal of Drug Policy*, 2021, **95**, 103197.
3. P. Sornsenee, S. Chimplee and C. Romyasamit, *Probiotics and Antimicrobial Proteins*, 2023, 1-13.
4. C. Stanciu, S. Ahmed, S. Gnanasegaram, S. Gibson, T. Penders, O. Grundmann and C. McCurdy, *The American Journal of Drug and Alcohol Abuse*, 2022, **48**, 509-528.
5. R. Hossain, A. Sultana, M. Nuinoon, K. Noonong, J. Tangpong, K. H. Hossain and M. A. Rahman, *Molecules*, 2023, **28**, 7372.
6. K. Phesatcha, B. Phesatcha, M. Wanapat and A. Cherdthong, *Fermentation*, 2022, **8**, 8.
7. F. Zakaria, J.-K. Tan, S. M. M. Faudzi, M. B. A. Rahman and S. E. Ashari, *Ultrasonics Sonochemistry*, 2021, **81**, 105851.
8. T. Petcharat, T. Sae-leaw, S. Benjakul, T. H. Quan, S. Indriani, Y. Phimolsiripol and S. Karnjanapratum, *Process Biochemistry*, 2024, **142**, 212-222.
9. S. Parthasarathy, J. B. Azizi, S. Ramanathan, S. Ismail, S. Sasidharan, M. I. M. Said and S. M. Mansor, *Molecules*, 2009, **14**, 3964-3974.
10. R. Yuniarti, S. Nadia, A. Alamanda, M. Zubir, R. Syahputra and M. Nizam, 2020.
11. M. Çam, N. C. İçyer and F. Erdoğan, *LWT-Food Science and Technology*, 2014, **55**, 117-123.
12. E. Dobroslavić, I. Elez Garofulić, Z. Zorić, S. Pedisić, M. Roje and V. Dragović-Uzelac, *Foods*, 2023, **12**, 1923.
13. S. Jafari, S. M. Jafari, M. Ebrahimi, I. Kijpatanasilp and K. Assatarakul, *Food hydrocolloids*, 2023, **134**, 108068.
14. S. Insang, I. Kijpatanasilp, S. Jafari and K. Assatarakul, *Ultrasonics Sonochemistry*, 2022, **82**, 105806.
15. S. Jafari, Z. Karami, K. A. Shiekh, I. Kijpatanasilp, R. W. Worobo and K. Assatarakul, *Foods*, 2023, **12**, 412.
16. M. Fikry, Y. A. Yusof, A. M. Al-Awaadh, R. A. Rahman and N. L. Chin, *Journal of Food Measurement and Characterization*, 2020, **14**, 1158-1171.
17. D. W. Dadi, S. A. Emire, A. D. Hagos and J.-B. Eun, *Industrial Crops and Products*, 2020, **156**, 112891.
18. V. Sablania, S. J. D. Bosco, S. Rohilla and M. A. Shah, *Journal of Food Measurement and Characterization*, 2018, **12**, 892-901.
19. D. W. Dadi, S. A. Emire, A. D. Hagos and J.-B. Eun, *Cogent Food & Agriculture*, 2019, **5**, 1690316.
20. A. Martinić, A. Kalušević, S. Lević, V. Nedović, A. Vojvodić Cebin, S. Karlović, I. Špoljarić, G. Mršić, K. Žižek and D. Komes, *Food technology and biotechnology*, 2022, **60**, 237-252.
21. A. Dobrinčić, L. Tuđen, M. Repajić, I. E. Garofulić, Z. Zorić, V. Dragović-Uzelac and B. Levaj, *Acta alimentaria*, 2020, **49**, 475-482.
22. E. González, A. M. Gómez-Caravaca, B. Giménez, R. Cebrián, M. Maqueda, A. Martínez-Férez, A. Segura-Carretero and P. Robert, *Food chemistry*, 2019, **279**, 40-48.
23. D. W. Dadi, S. A. Emire, A. D. Hagos and J.-B. Eun, *Annals: Food Science & Technology*, 2019, **20**.
24. C. Tongped and N. Trongsiriwat, King Mongkut's University of Technology North Bangkok, 2025.

View Article Online
DOI: 10.1039/D5FB00648A

25. M. Matra, S. Phupaboon, P. Totakul, R. Prommachart, A. A. Shah, A. M. Shah and M. Wanapat, *Animal bioscience*, 2023, **37**, 74.
26. M. Matra, S. Phupaboon, P. Totakul, R. Prommachart and M. Wanapat, *International Journal of Agriculture and Biosciences*, 2025, **14**, 258-264.
27. M. Fikry, S. Jafari, K. A. Shiekh, I. Kijpatanasilp, S. Khongtongsang, E. Khojah, H. A. A. L. Jumayi and K. Assatarakul, *Ultrasonics Sonochemistry*, 2024, DOI: https://doi.org/10.1016/j.ultsonch.2024.106949, 106949.
28. M. Sharma and K. K. Dash, *Innovative Food Science & Emerging Technologies*, 2022, **75**, 102913.
29. Y. Ramakrishnan, N. M. Adzahan, Y. A. Yusof and K. Muhammad, *Powder technology*, 2018, **328**, 406-414.
30. K. Slinkard and V. L. Singleton, *American journal of enology and viticulture*, 1977, **28**, 49-55.
31. S. Chheng, M. Fikry, S. Jafari, D. K. Mishra and K. Assatarakul, *Journal of Stored Products Research*, 2025, **112**, 102660.
32. M. Fikry, Y. A. Yusof, A. M. Al-Awaadh, R. A. Rahman, N. L. Chin, E. Mousa and L. S. Chang, *Food Science and Technology Research*, 2019, **25**, 351-362.
33. M. Ahmed, M. S. Akter and J. B. Eun, *Journal of the Science of Food and Agriculture*, 2010, **90**, 494-502.
34. L. Wen, B. Yang, C. Cui, L. You and M. Zhao, *Food Analytical Methods*, 2012, **5**, 1244-1251.
35. S. Chheng and K. Assatarakul, Summer Institute of Asia & ASEAN Center for Educational Research, Chiba University, Japan, 2023.
36. K. Papoutsis, P. Pristijono, J. B. Golding, C. E. Stathopoulos, M. C. Bowyer, C. J. Scarlett and Q. V. Vuong, *Journal of Food Processing and Preservation*, 2017, **41**, e13152.
37. M. Fikry, S. Jafari, K. A. Shiekh, I. Kijpatanasilp, S. Chheng and K. Assatarakul, *Food and Bioprocess Technology*, 2024, DOI: 10.1007/s11947-024-03421-0, 1-18.
38. S. Chheng, S. Jafari, D. Mishra and K. Assatarakul, *Sustainable Food Technology*, 2025, DOI: 10.1039/D5FB00227C.
39. P. Siddhuraju and S. Manian, *Food chemistry*, 2007, **105**, 950-958.
40. I. Atalar and M. Dervisoglu, *LWT-Food Science and Technology*, 2015, **60**, 751-757.
41. R. K. Cruz-Bravo, D. Guajardo-Flores, C. A. Gómez-Aldapa, J. Castro-Rosas, R. O. Navarro-Cortez, L. Díaz-Batalla and R. N. Falfán-Cortés, *CyTA-Journal of Food*, 2023, **21**, 493-501.
42. M. Fikry, R. Sami, A. A. Al-Mushhin, A. H. Aljahani, A. Almasoudi, S. Alharthi, K. A. Ismail and M. Dabbour, *Journal of Biobased Materials and Bioenergy*, 2022, **16**, 150-158.
43. D. Gómez-Díaz, J. M. Navaza and L. Quintáns-Riveiro, *International Journal of Food Properties*, 2008, **11**, 773-780.
44. P. Pittia and M. Faieta, in *Spray Drying Encapsulation of Bioactive Materials*, CRC Press, 2021, pp. 355-376.
45. K. Simon-Brown, K. M. Solval, A. Chotiko, L. Alfaro, V. Reyes, C. Liu, B. Dzandu, E. Kyereh, A. G. Barnaby and I. Thompson, *LWT*, 2016, **70**, 119-125.
46. W. Ren, G. Tian, S. Zhao, Y. Yang, W. Gao, C. Zhao, H. Zhang, Y. Lian, F. Wang and H. Du, *Lwt*, 2020, **133**, 109954.
47. T. T. Tran and H. V. Nguyen, *Beverages*, 2018, **4**, 84.
48. C. T. Nguyen, K. N. Di, H. C. Phan, T. C. Kha and H. C. Nguyen, *International Journal of Biological Macromolecules*, 2024, **269**, 132217.
49. T. P. Labuza and B. Altunakar, *Water activity in foods: fundamentals and applications*, 2020, 161-205.
50. J. Astina and S. Sapwarobol, *Journal of the American College of Nutrition*, 2019, **38**, 380-385.
51. S. Y. Quek, N. K. Chok and P. Swedlund, *Chemical Engineering and Processing: Process Intensification*, 2007, **46**, 386-392.
52. P. Mishra, S. Mishra and C. L. Mahanta, *Food and bioproducts processing*, 2014, **92**, 252-258.

View Article Online
DOI: 10.1039/D5FB00648A

53. R. V. de Barros Fernandes, S. V. Borges and D. A. Botrel, *Carbohydrate polymers*, 2014, **101**, 524-532.
54. E. J. G. Laureanti, T. S. Paiva, L. M. de Matos Jorge and R. M. M. Jorge, *International journal of biological macromolecules*, 2023, **253**, 126969.
55. S. B. Nimse and D. Pal, *RSC advances*, 2015, **5**, 27986-28006.
56. V. M. Silva, L. E. Kurozawa, K. J. Park and M. D. Hubinger, *Drying Technology*, 2012, **30**, 175-184.
57. C. Cao, X. Zhao, C. Zhang, Z. Ding, F. Sun and C. Zhao, *Journal of Food Science*, 2020, **85**, 3442-3449.
58. E. M. Mudge and P. N. Brown, *Journal of AOAC International*, 2017, **100**, 18-24.
59. N. Isnaeni, A. Saefumillah and A. H. Cahyana, *Eruditio: Indonesia Journal of Food and Drug Safety*, 2024, **4**, 130-144.
60. A. Al-Hamayda, B. Abu-Jdayil, M. Ayyash and J. Tannous, *Industrial Crops and Products*, 2023, **205**, 117556.
61. E. Díaz-Montes, *Polymers*, 2023, **15**, 2659.
62. D. A. Pai, V. R. Vangala, J. W. Ng, W. K. Ng and R. B. Tan, *Journal of Food Engineering*, 2015, **161**, 68-74.
63. H. C. Carneiro, R. V. Tonon, C. R. Grosso and M. D. Hubinger, *Journal of food engineering*, 2013, **115**, 443-451.
64. A. Tolun, Z. Altintas and N. Artik, *Journal of biotechnology*, 2016, **239**, 23-33.
65. L. Alamilla-Beltran, J. J. Chanona-Perez, A. R. Jimenez-Aparicio and G. F. Gutierrez-Lopez, *Journal of Food Engineering*, 2005, **67**, 179-184.
66. Z. Zhang, S. Zhang, R. Su, D. Xiong, W. Feng and J. Chen, *Journal of food science*, 2019, **84**, 1427-1438.
67. R. Vehring, H. Snyder and D. Lechuga-Ballesteros, *Drying technologies for biotechnology and pharmaceutical applications*, 2020, 179-216.
68. R. Chedoloh and S.-a. Asae, *Burapha Science Journal*, 2017, 78-91.
69. A. Dutta and G. Dutta, *Journal of Applied Packaging Research*, 2016, **8**, 5.
70. S. N. Dirim and G. Çalışkan, 2012.
71. C. Wong and W. Lim, *International Food Research Journal*, 2016, **23**, 1887.
72. O. Jiménez-González and J. Á. Guerrero-Beltrán, *Food Engineering Reviews*, 2021, **13**, 769-811.
73. S. C. de Moura, C. L. Berling, A. O. Garcia, M. B. Queiroz, I. D. Alvim and M. D. Hubinger, *Food Research International*, 2019, **121**, 542-552.
74. R. V. Tonon, C. Brabet and M. D. Hubinger, *Journal of food engineering*, 2008, **88**, 411-418.
75. J. K. Agbenorhevi and L. J. Marshall, *Journal of Food Science and Engineering*, 2012, **2**, 72.
76. S. Agustini and M. K. Yusya, *Current Research on Biosciences and Biotechnology*, 2020, **1**, 66-70.
77. C. Baltacioğlu, S. Velioğlu and E. Karacabey, *Journal of Food Quality*, 2011, **34**, 278-283.
78. M. Thakur and V. Nanda, *Food Chemistry Advances*, 2024, **4**, 100567.
79. S. Warnasih and U. Hasanah, *Journal of Science Innovare*, 2019, **1**, 44-49.
80. T. Okuda and H. Ito, *Molecules*, 2011, **16**, 2191-2217.
81. K. Jitrangsri, A. Chaidedgumjorn and M. Satiraphan, *Pharmaceutical Sciences Asia*, 2020, **47**, 164-172.
82. S. C. Foo, F. M. Yusoff and N. M. Khong, *Journal of Agriculture and Food Research*, 2024, **15**, 100823.
83. C. Bustos-Garza, J. Yáñez-Fernández and B. E. Barragán-Huerta, *Food Research International*, 2013, **54**, 641-649.
84. S. A. Desobry, F. M. Netto and T. P. Labuza, *Journal of food science*, 1997, **62**, 1158-1162.

View Article Online
DOI: 10.1039/D5FB00648A

Figures

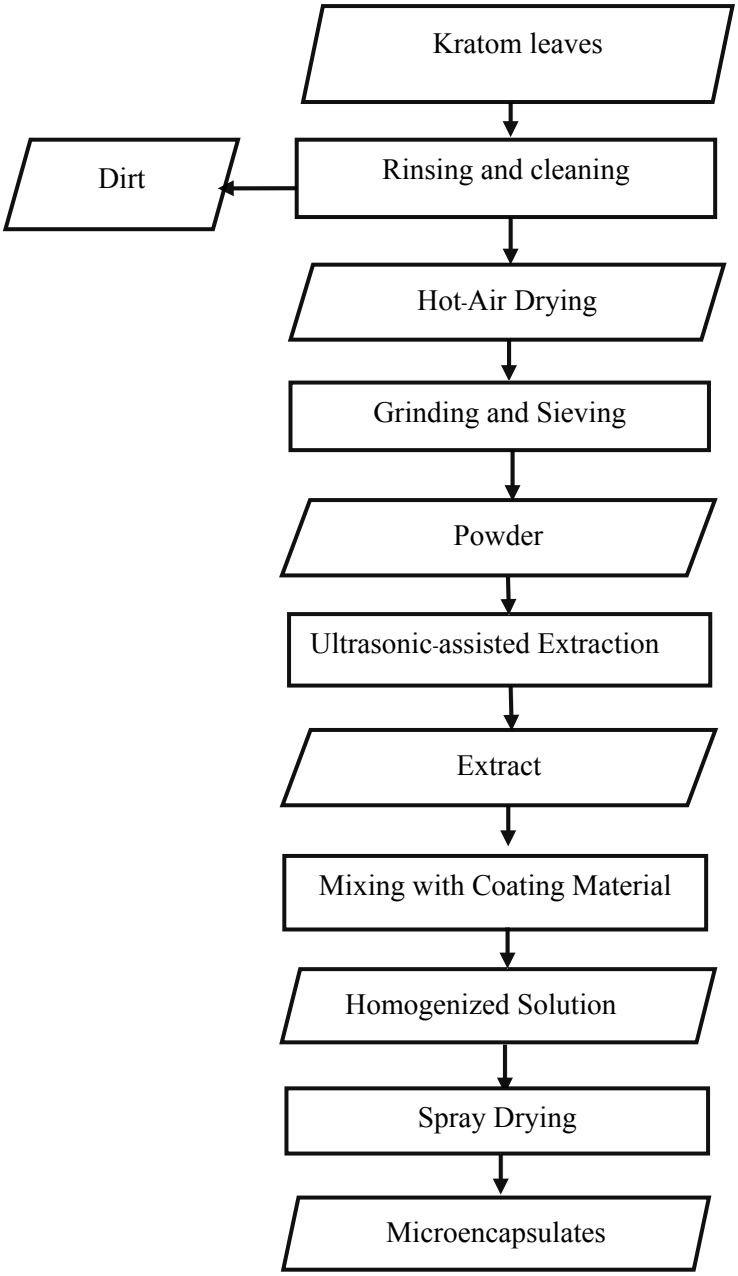

Figure 1. Production flow chart of KLE microcapsules of bioactive compounds extracted from kratom leaves.

View Article Online
DOI: 10.1039/D5FB00648A

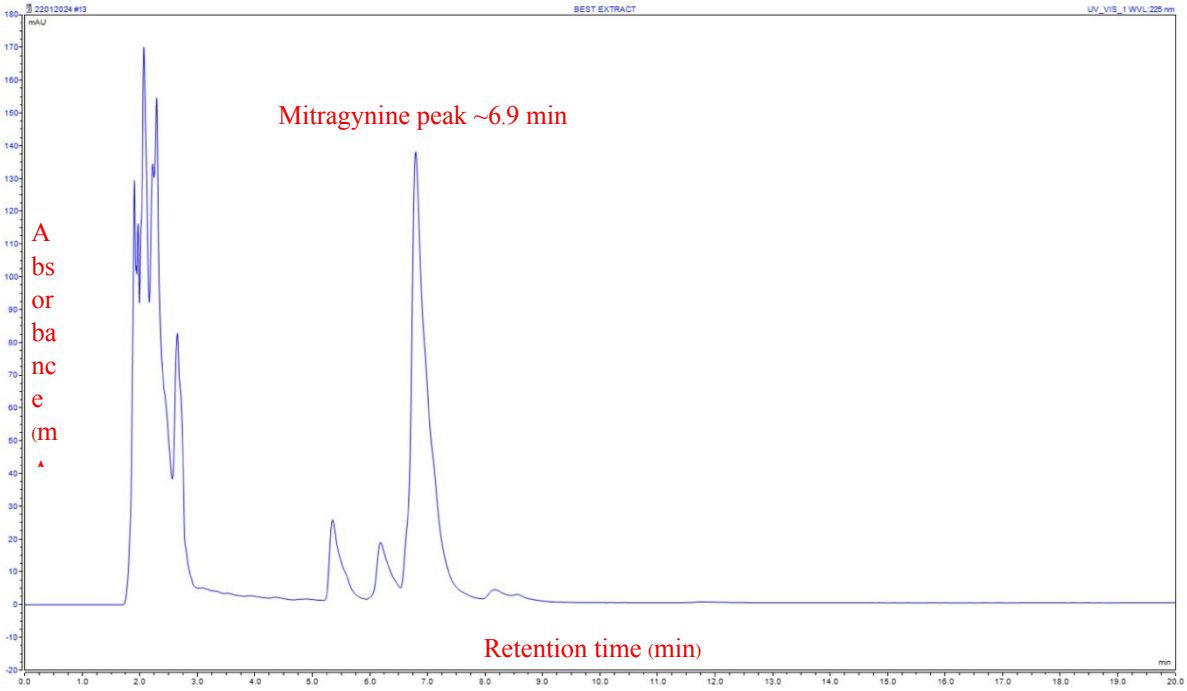

Figure 2. HPLC chromatogram of Kratom leaf extract (KLE), showing the major alkaloid mitragynine at a retention time of approximately 6.9 min and minor peaks corresponding to other alkaloids and phenolic compounds. X-axis: Retention time (min); Y-axis: Absorbance (mAU).

View Article Online
DOI: 10.1039/D5FB00648A

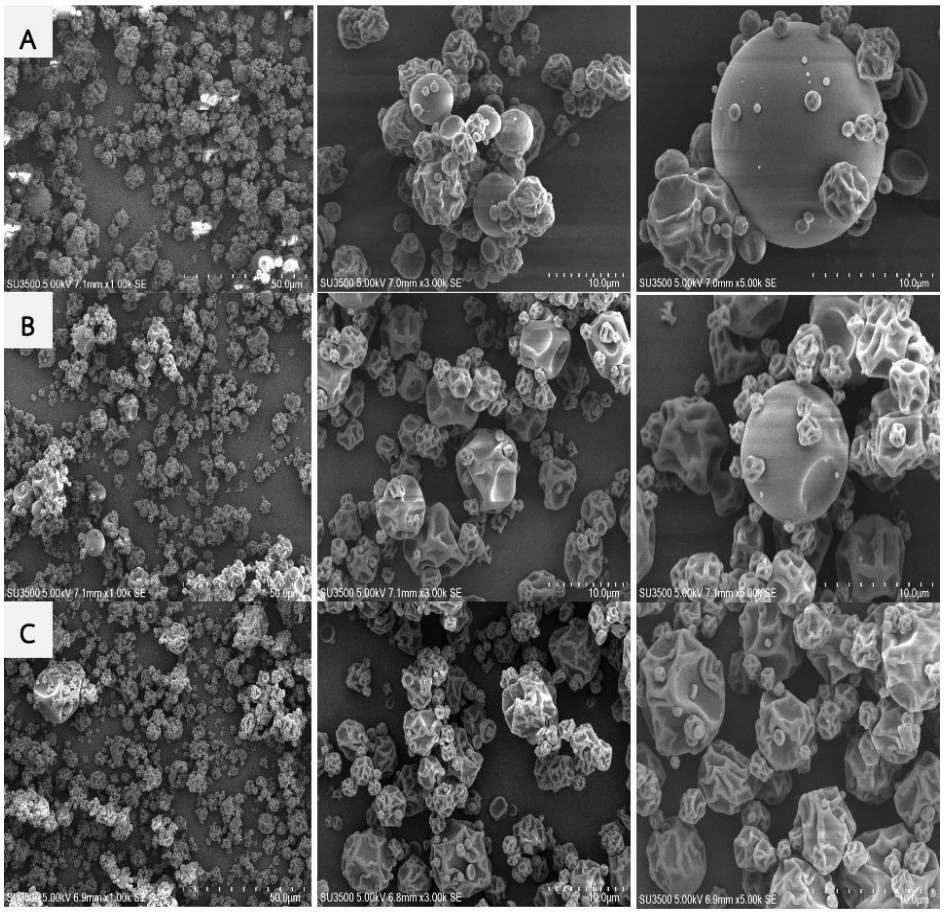

Figure 3. Scanning electron microscopy images at magnifications of 1,000x, 3,000x, and 5,000x (left to right) of KLE microcapsules obtained at an inlet temperature of 150°C: (A) coated with resistant maltodextrin DE10, (B) coated with gum Arabic, and (C) coated with a 1:1 ratio of resistant maltodextrin and gum Arabic.

View Article Online
DOI: 10.1039/D5FB00648A

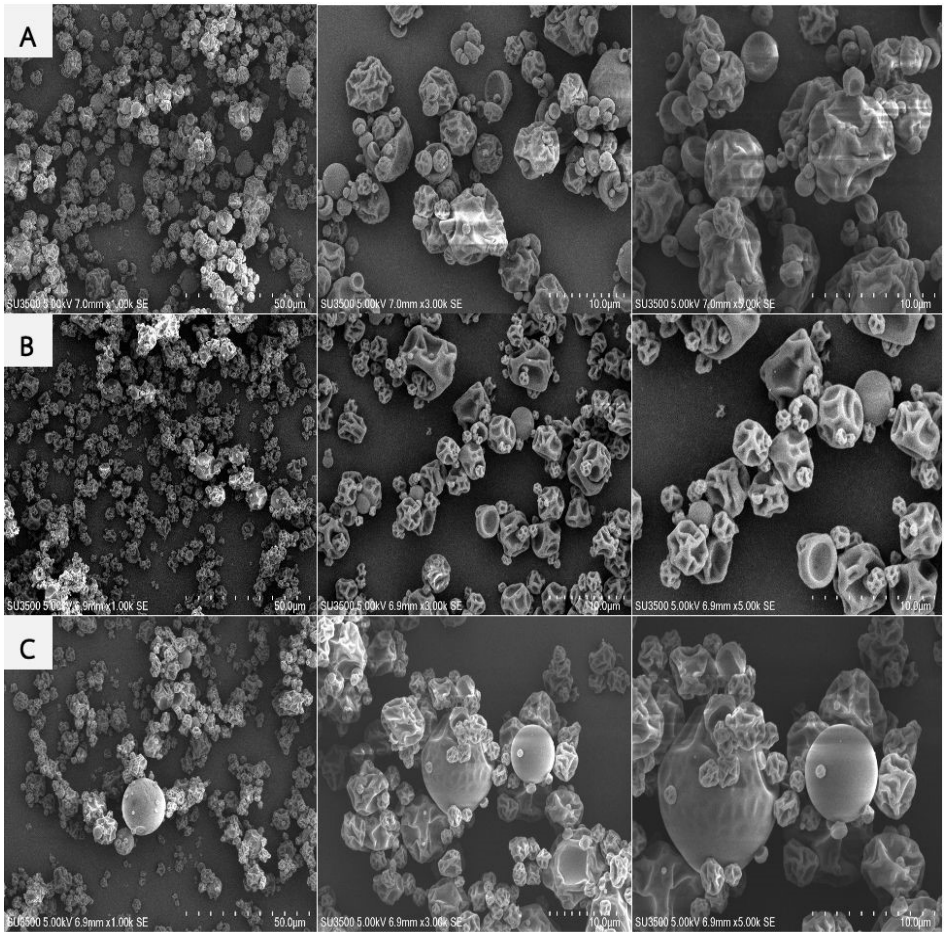

Figure 4. Scanning electron microscopy images at magnifications of 1,000×, 3,000×, and 5,000× (left to right) of KLE microcapsules obtained at an inlet temperature of 160 °C: (A) coated with resistant maltodextrin DE10, (B) coated with gum Arabic, and (C) coated with a 1:1 ratio of resistant maltodextrin and gum Arabic.

View Article Online
DOI: 10.1039/D5FB00648A

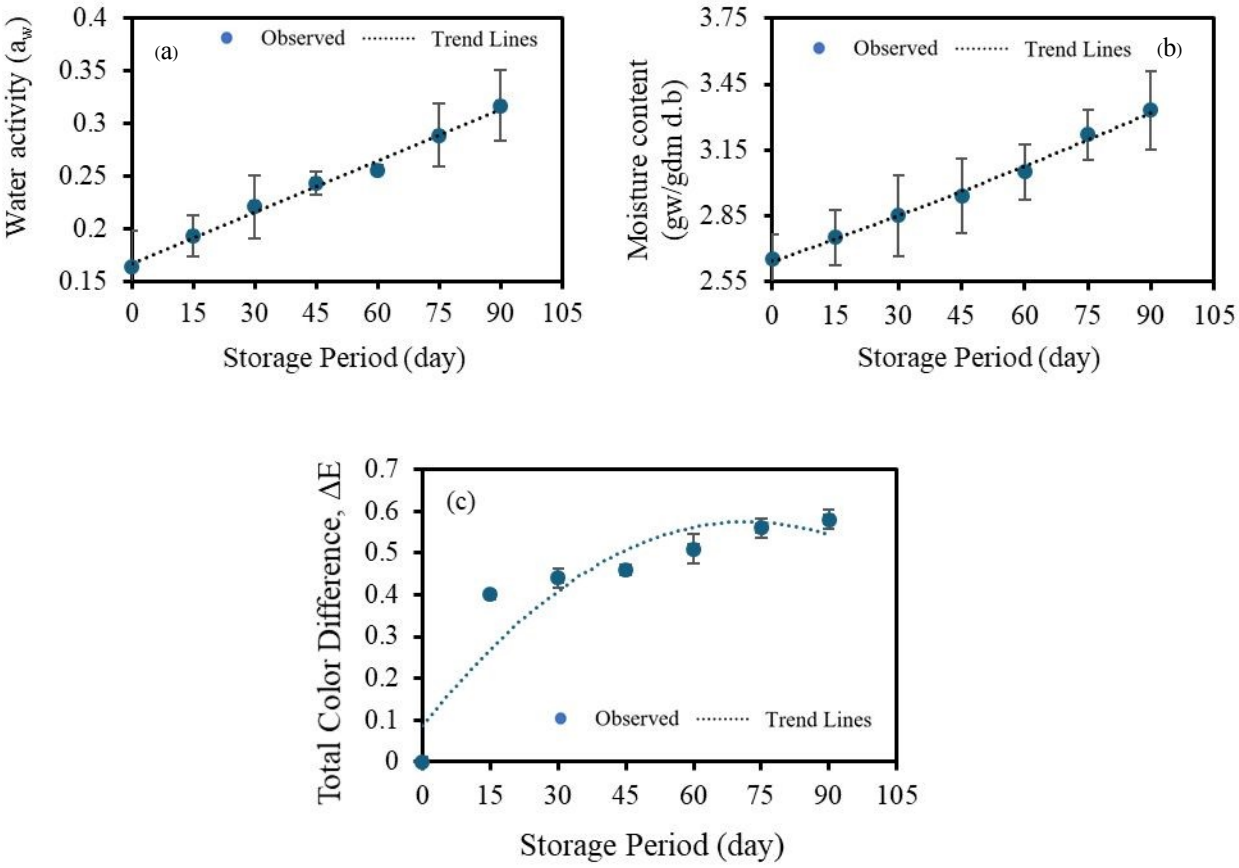

Figure 5. Moisture content (a), water activity (b), and total color difference (c) of stored KLE microcapsules at different storage periods. Values represent means ± SD (n = 3).

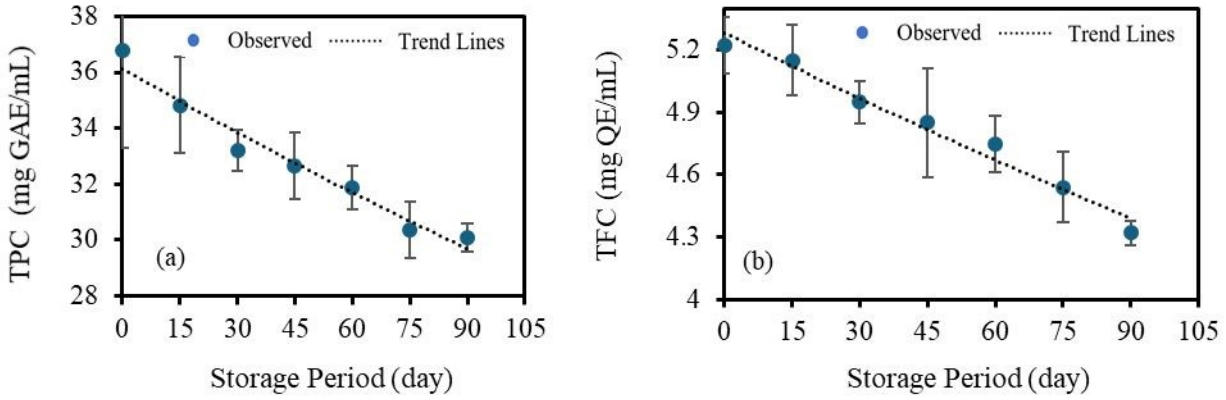

View Article Online
DOI: 10.1039/D5FB00648A

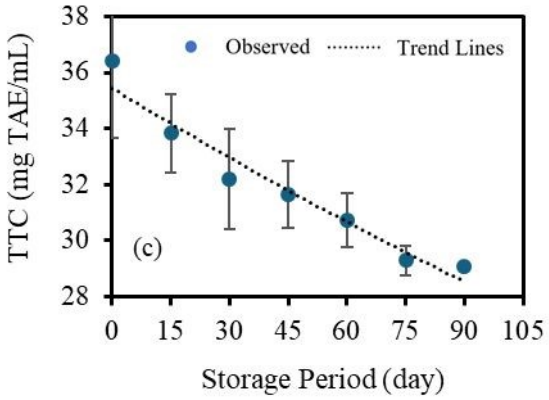

Figure 6. Total phenolic content (TPC, a), total flavonoid content (TFC, b), and total tannin content (TTC, c) of stored KLE microcapsules at different storage periods. Values represent means ± SD (n = 3).

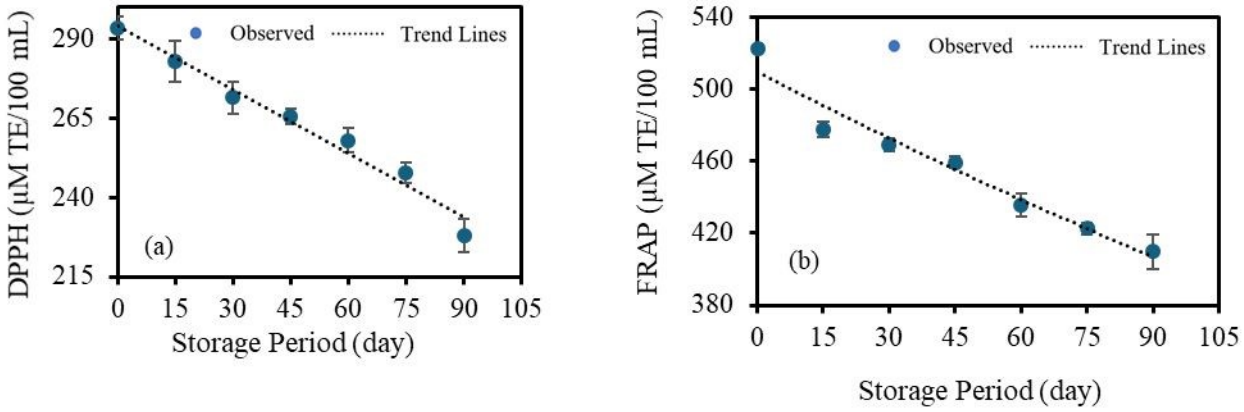

Figure 7. Antioxidant activities of stored KLE microcapsules measured by (a) DPPH radical-scavenging assay and (b) FRAP assay. Values represent means ± SD (n = 3). DPPH = 2,2-diphenyl-1-picrylhydrazyl; FRAP = ferric-reducing antioxidant power.

View Article Online
DOI: 10.1039/D5FB00648A

Tables

Table 1
Production conditions of KLE microcapsules using spray drying

Experiment	Inlet Temperature	Type of Coating Material	KLE to Coating Material Ratio (w/w)
1	150°C	40% Resistant Maltodextrin	1:2
2		20% Gum Arabic	1:2
3		40% Resistant Maltodextrin with 20% Gum Arabic (1:1 ratio)	1:2
4	160°C	40% Resistant Maltodextrin	1:2
5		20% Gum Arabic	1:2
6		40% Resistant Maltodextrin with 20% Gum Arabic (1:1 ratio)	1:2

Table 2.
Mean Values of physicochemical properties of kratom leaf extract microcapsules as affected by different wall materials and inlet temperatures.

Property	Inlet Temperature (°C)	40% Resistant Maltodextrin	20% Gum Arabic	40% Resistant Maltodextrin + 20% Gum Arabic (1:1)	Carrier η^2	Temperature η^2	Interaction η^2
Yield (%)	150	72.85 ± 1.08 Aa	58.24 ± 0.60 Aa	67.52 ± 0.83 Aa	0.28	0.07	0.05
	160	63.61 ± 3.81 Aa	65.23 ± 3.54 Aa	66.26 ± 0.98 Aa			
EE (%)	150	79.34 ± 2.88 ABa	67.87 ± 1.50 Aa	67.52 ± 0.89 Aa	0.35	0.18	0.09
	160	59.16 ± 5.26 ABa	84.65 ± 1.32 Aa	62.45 ± 2.53 Aa			
Water solubility (%)	150	95.55 ± 0.26 Ba	91.82 ± 0.09 Aa	93.21 ± 0.26 Aa	0.22	0.1	0.04
	160	95.34 ± 0.58 Bb	95.10 ± 0.48 Ab	94.75 ± 0.38 Ab			
Moisture content (%)	150	2.59 ± 0.09 Aa	6.81 ± 0.15 Aa	2.90 ± 0.07 Aa	0.15	0.27	0.07
	160	3.52 ± 0.07 Aa	2.67 ± 0.10 Aa	3.30 ± 0.13 Aa			
Water activity	150	0.23 ± 0.00 Aa	0.26 ± 0.04 Aa	0.18 ± 0.22 Aa	0.08	0.12	0.03
	160	0.21 ± 0.01 Aa	0.16 ± 0.03 Aa	0.22 ± 0.02 Aa			
L-value*	150	64.32 ± 1.19 Ca	60.76 ± 0.88 Aa	62.80 ± 0.85 Ba	0.19	0.14	0.06
	160	64.80 ± 1.24 Cb	60.41 ± 1.12 Aa	63.05 ± 0.67 Bb			
a-value*	150	-1.29 ± 0.02 Db	-0.44 ± 0.06 Aa	-0.51 ± 0.07 Ba	0.24	0.1	0.05
	160	-1.24 ± 0.01 Da	-0.47 ± 0.04 Aa	-0.63 ± 0.08 Ca			
b-value*	150	4.07 ± 0.12 Aa	7.62 ± 0.34 Bb	6.67 ± 0.76 Db	0.32	0.12	0.08

View Article Online
DOI: 10.1039/D5FB00648A

	160	4.17 ± 0.87 Aa	8.09 ± 0.83 Bc	8.25 ± 0.43 Dc			
TPC	150	13.07 ± 2.13 Ba	25.91 ± 1.45 Aa	17.14 ± 0.30 Aa	0.29	0.16	0.1
	160	15.71 ± 0.65 Ba	34.75 ± 2.66 Aa	25.62 ± 2.21 Aa			
TTC	150	13.39 ± 2.34 Aa	27.59 ± 1.58 a	17.11 ± 0.63 Aa	0.25	0.2	0.12
	160	18.66 ± 1.41 Ab	35.46 ± 2.87 b	26.07 ± 1.50 Ab			
TFC	150	1.79 ± 0.20 Ca	4.84 ± 0.50 Aa	2.92 ± 0.23 Ca	0.3	0.14	0.09
	160	1.98 ± 0.40 Ca	5.05 ± 0.06 Aa	3.18 ± 0.23 Ca			
DPPH	150	243.54 ± 4.10 Ca	279.93 ± 1.64 Aa	233.54 ± 3.09 Ca	0.27	0.18	0.08
	160	239.72 ± 6.05 Ca	305.24 ± 2.59 Aa	238.78 ± 1.11 Ca			
FRAP	150	343.56 ± 3.12 Aa	400.52 ± 2.01 Aa	413.99 ± 2.33 Aa	0.33	0.21	0.11
	160	322.29 ± 4.59 Aa	522.74 ± 2.47 Aa	317.48 ± 8.14 Aa			
Mitragynine	150	0.96 ± 0.09 Ca	1.89 ± 0.06 Aa	1.36 ± 0.09 Ca	0.21	0.09	0.05
	160	1.06 ± 0.02 Ca	1.96 ± 0.04 Aa	1.38 ± 0.09 Ca			

Values are presented as mean ± SD (n = 3). Different uppercase letters within the same row indicate significant differences ($p < 0.05$) among wall materials. Different lowercase letters within the same column indicate significant differences ($p < 0.05$) between temperatures. Means sharing the same letter are not significantly different according to Tukey's HSD test.

Table 3.

Statistical parameters of the models used in the study and the predicted shelf life of KLE microcapsules using GA at 160 °C.

Properties	Parameter	Zero-order model		First-order model		Predicted Shelf life (day)
		Values	CI (95%)	Values	CI (95%)	
Moisture content (%)	Co	2.629	(2.58,2.68)	2.639	(2.61,2.67)	92.55
	k	-0.008	(-0.008,-0.007)	-0.003	(-0.003,-0.002)	
	R^2		0.991		0.995	
Water activity	Co	0.167	(0.158,0.176)	0.174	(0.163,0.185)	91.88
	k	-0.002	(-0.002,-0.001)	-0.007	(-0.008,-0.006)	
	R^2		0.992		0.986	
TPC (mg GAE/g db.)	Co	36.076	(35.14,37.02)	36.193	(35.32,37.07)	82.84
	k	0.072	(0.055,0.089)	0.002	(0.002,0.003)	
	R^2		0.958		0.966	
TTC (mg TAE/g db.)	Co	35.378	(34.13,36.63)	35.528	(34.35,36.7)	81.26
	k	0.078	(0.054,0.10)	0.002	(0.002,0.003)	
	R^2		0.937		0.949	
TFC (mg QE/g db.)	Co	5.267	(5.18,5.36)	5.275	(5.17,5.38)	96.55
	k	0.010	(0.008,0.011)	0.002	(0.0016,0.0024)	
	R^2		0.978		0.972	
DPPH (μM TE/100g db.)	Co	294.014	(287.14,300.89)	294.743	(286.74,302.75)	98.77

View Article Online
DOI: 10.1039/D5FB00648A

	k	0.670	(0.54,0.80)	0.003	(0.002,0.003)	
	R^2		0.973		0.967	
FRAP (μM TE/100g db.)	Co	508.397	(491.3,525.17)	510.410	(494.2,526.6)	85.90
	k	1.149	(0.84,1.46)	0.003	(0.0019,0.0032)	
	R^2		0.948		0.955	
Integrated shelf-life decision (minimum across attributes)	-		-		-	**81.26**

View Article Online
DOI: 10.1039/D5FB00648A

Data availability Statement

The data supporting the findings of this study are available from the corresponding author upon request.